IEEE Access
Multidisciplinary ⋮ Rapid Review ⋮ Open Access Journal

Received February 4, 2019, accepted February 26, 2019, date of publication March 7, 2019, date of current version May 22, 2019.

Digital Object Identifier 10.1109/ACCESS.2019.2903453

Performance Analysis of Full-Duplex Vehicle Relay-Based Selection in Dense Multi-Lane Highways

KHALED ESHTEIWI[1], GEORGES KADDOUM[1], (Member, IEEE), KAIS BEN FREDJ[2], (Member, IEEE), EBRAHIM SOUJERI[1], (Senior Member, IEEE), AND FRANÇOIS GAGNON[1], (Senior Member, IEEE)

[1]LaCIME Laboratory, École de Technologie Supérieure, University of Quebec, Montreal, QC H3C 1K3, Canada
[2]IRNS, University of Quebec, Montreal, QC H5A 1J6, Canada

Corresponding author: Khaled Eshteiwi (khaled-mohamed.eshteiwi.1@ens.etsmtl.ca)

ABSTRACT This paper considers a dual-hop vehicle-to-vehicle (V2V) communication system equipped with full-duplex relays (FDRs) in the millimeter-wave networks. The performance of this network is studied in a dense multi-lane highway considering cooperative best vehicular relay selection strategy. In fact, two different FDR schemes are analyzed for the given network. In the first scheme that is called self-interference (SI) vehicle relaying selection, the FDR models the source–relay and the relay–relay links by one channel state information (CSI) coefficient (i.e., a single channel estimation of the two links), while in the second scheme that is called individual SI vehicle relaying selection, the CSI of the source–relay and the relay–relay links are estimated separately. Moreover, relay–destination link is modeled by one CSI coefficient in both aforementioned schemes. Dissimilar to traditional V2V schemes where either line-of-sight (LOS) or non-line-of-sight (NLOS) propagation is considered, and the effect of the blockage on V2V communications is not taken into account when analyzing the performance, in this paper, we propose a probabilistic model capturing the occurrences of LOS and NLOS propagations, which depend on the movement of the vehicles between the central and adjacent lanes. Thus, the movement of the vehicles between any two adjacent lanes is assumed to take place independently and is deemed to be according to the Poisson distribution. This vehicle movement model considers the blockage between the source and destination links. In this vein, a LOS link is considered available when the center lane is clear of vehicles between the source and destination nodes, and an NLOS link is assumed otherwise. Furthermore, a Nakagami-m fading channel model is considered due to its excellent representation of the V2V communication environment. The LOS/NLOS probabilities combined together with the probability of blockage are used to analyze the system performance. The cumulative density function expression of the signal-to-interference-plus-noise ratio at the relay is derived for both relaying schemes. Moreover, the lower bound expressions of the end-to-end outage probabilities are developed and used to express throughput. Finally, the theoretical results postulated and presented here are verified by the numerical simulation for a variety of parameters.

INDEX TERMS Full duplex relaying, V2V communications, relay selection, Nakagami$-m$ fading channel, outage probability, throughput, blockage probability.

I. INTRODUCTION

The growth and expansion of intelligent transportation technologies for the next generation vehicular communications have brought with them a few key challenges. Focusing on inter-vehicle congestions during heavy traffic or accidents, an ultra-low latency transmission is vital to send ultra-fast warning messages within an extremely short time frame [1]. This is because the inter-connected and autonomous vehicles of the future will need to exchange information at a high data rate and low latency. In this context, emerging technologies have recently used mmWave frequency bands

The associate editor coordinating the review of this manuscript and approving it for publication was Quansheng Guan.

between 30 GHz and 300 GHz to provide an alternative solution in order to offer both high data rates, of up to 7 Gbps, and low latency of less than 10 msec [2], [3]. Some of the key features of advanced vehicular applications under the umbrella of intelligent transportation systems (ITSs) can be exploited to offer passengers smart applications, including vehicle parking, accident response, traffic congestion and accident avoidance tools [4]. Based on the aforementioned applications, the enhancement of the currently ongoing systems capacity and the incremental growth of data rates are extremely important, and are therefore, being explored as part of the fifth-generation (5G) standardization effort by third Generation Partnership Project (3GPP). One of the key areas to explore under 5G is vehicular cooperative wireless [5], wherein the objectives are to reduce the aftermath of multi-path fading and signal degradation within the vehicular wireless communications space. Likewise, cooperative relaying systems based on V2V communications, also known as inter-vehicular communications (IVC), increase the diversity and generally improve the performance of wireless communication systems.

In addition, the cooperation mechanism between vehicles and infrastructure can be improved by extending the technology to enhance the coverage area, thereby offering improved road safety and better network connectivity [6]. One of the key solutions to this requirement is the implementation of full duplex relaying in order to reduce the end-to-end delay and to concurrently double the spectral efficiency when self-interference is eliminated [7]. This is because with full duplex, also known as in-band full duplex, the relays avoid any spectral efficiency loss by transmitting and receiving over the same band simultaneously. However, a full duplex relaying performance could be severely degraded, because of the self-interference at the relay node due to the simultaneous transmission and reception over the same channel, which cannot be perfectly eliminated [8], [9]. Meanwhile, in the half duplex relaying, also known as out-of-band full duplex, the relays encounter a spectral efficiency loss as they transmit and receive in different time slots and over different frequency bands. As a result, in practical FDR protocol designs, the impact of self-interference should be taken into account for a more accurate system analysis.

Recently, N^* Nakagami fading channels in cooperative wireless communications have been proposed and analyzed in many scenarios and under different cooperative relaying techniques. Qin *et al.* [10] studied the average symbol error probability for a cooperative system that contains a single source node, a single destination node and a single relay for amplify-and-forward (AF) relaying over Nakagami-m fading channels by implementing various modulation techniques. The cellular multiuser two-way relay network has been evaluated in terms of the outage probability under Nakagami-m fading [11], where a multi-antenna base station communicates bidirectionally, i.e. in a full duplex mode, with several single-antenna mobile stations via a single-antenna relay node. Such systems can accomplish both multi-user diversity and multi-antenna diversity. The outage probability and average symbol error rate are derived for orthogonal frequency division multiplexing (OFDM) over independent but non-identical Nakagami-m distributed fading channels [12]. Moreover, cooperative AF relaying with a non-linear power amplifier is considered at the relay terminal. Qian *et al.* [13] have shown that the lossy forward (LF) relaying scheme outperforms the conventional decode-and-forward (DF) relaying in terms of outage probability over Nakagami-m fading environments.

Recent works on full duplex unidirectional and bidirectional wireless cooperative relaying schemes, including self-interference were studied and analyzed in different communication scenarios in [14]–[21]. In addition, a bidirectional full duplex mode is investigated for a single relay in [22] and for multi-relays in [23]. The performance of full duplex DF relay selection over Nakagami-m fading channels is investigated and analyzed in term of outage probability in [24].

A study of FDR with improper Gaussian signaling (IGS) is presented in [25], in which the authors show that IGS is superior to proper Gaussian signaling (PGS) in terms of interference-limited settings. Moreover, the outage probability and the ergodic rate are derived to evaluate the system performance. The performances of FDR over a Nakagami-m fading environment is presented in [26], where, the outage probability of hybrid automatic repeat requests (ARQs) is derived. Fu *et al.* [27] have derived approximate probability density functions (PDFs) for double-Nakagami fading and Gamma-Gamma fading channels. The approximated PDF is then used to determine the outage probability, the ergodic capacity and the symbol error rate for the equal-gain and selection combining diversity techniques.

From the vehicular communication perspective, several V2V half-duplex relaying (HDR) techniques have been studied and investigated in the literature. The communication between source-destination (S-D) nodes could be established by a road access point (AP) [28], a mobile vehicle [29] and multiple mobile vehicles in [30]. Ilhan *et al.* [31] studied two different cooperative relaying schemes. In the first scheme, V2V is assisted by an AP, and in the second one, V2V is assisted by relaying vehicles. Moreover, Nguyen and Kong [32] present a V2V dual-hop cooperative network under DF relaying scheme, where the communication between the two vehicles is assisted by the vehicles within one cluster and by APs in adjacent clusters, where the APs act as relays. Within the scope of V2V cooperative communications, the impacts of co-channel interference and imperfect channel estimation are studied in [33] and [34]. The performance of multi-hop V2V wireless cooperative communications over n^* Rayleigh fading channels is considered in [35], and a V2V multiple-input and multiple-output (MIMO) channel model is investigated in [36]. Additionally, a two-way HDR V2V wireless communication scheme over double-Rayleigh fading channels is proposed in [37], and over mixed Nakagami$-m$ and double Nakgamai$-m$

channels in [38]. The performance of V2V communication in a single dense lane topology is examined in [39], while [40] proposes a multi-lane topology with different packet forwarding schemes. In [41], an exact expression for the PDF of peer-to-peer V2V communication including the impact of interference is derived and used to obtain the bit error rate (BER).

Overall, *full duplex relaying* in vehicular communication is still in its infancy and very few works have been published, especially from the physical layer and performance analysis perspectives. Therefore, the current literature is limited to the V2V half-duplex scenario, except for the case of [42], where the authors present the simulation results of a V2V full duplex relay selection wireless cooperative communication by using joint decoding as proposed in [43], however, a mathematical analysis of the system performance is not included. Bazzi *et al.* [44] investigate the long term evolution (LTE) technique for V2V beaconing services by exploiting full duplex direct communications, while the joint resource assignment and power allocation problems are analyzed for full duplex vehicular communication from a medium access control (MAC) layer perspective in [45].

Our paper is a continuation, as well as an update, of the recent progress of IVC-based full duplex relaying. Thus, we consider a dual-hop full duplex V2V wireless cooperative communication in which a source vehicle (S) communicates with a destination vehicle (D) both directly and with the help of multiple cooperative vehicles-based on the full duplex relays present in the network. The analysis is performed for a dense multi-lane highway scenario in a non-regenerative AF relaying mode. Two relaying selection schemes are considered for such networks, and the availability of the CSI at the receiver side is assumed. Thereupon, to ensure good cooperation, the FDR represents the source-relay and the relay-relay links by one CSI coefficient for estimation process in the first scheme, which is the SI vehicle relaying selection, while for the second scheme,[1] which is the ISI vehicle relaying selection, the CSIs of the source-relay and of the relay-relay are estimated separately. In addition, a selection combining (SC) technique is employed to select the best vehicle relay that achieves the highest signal-to-noise ratio (SNR).

To create more realistic V2V communication scenarios, LOS and NLOS propagations between S and D are considered and the dependence of the probabilistic model on the movement of the vehicle between the central and adjacent lanes is studied. In fact, due to the unceasing movement of vehicles between adjacent lanes, which can be modeled based on independent vehicles Poisson distribution, the LOS is attainable *only* if the central lane between the source and the destination nodes is free of vehicles, otherwise, the NLOS dominates. Moreover, the intensity of the vehicles in each traffic lane is set according to an independent one-dimensional Poisson point process (PPP). It should be mentioned that the channels are modeled as Nakagami$-m$ fading channels for accuracy in modeling short-range highway vehicular communications. For the considered network model, the CDF expression of the source-relay link including self-interference is first derived, then the end-to-end lower bound outage probability is expressed in terms of the blockage probability in the central lane, and then the throughput is calculated and presented accordingly.

Based on the results obtained, the concept of multiple vehicular relays both offers diversity and significantly boosts performance by reducing the outage probability, which motivates its use in V2V environments. On the other hand, the essential differences between this work and the related work done in [40] are that in our work we consider a two-hop full duplex relaying over mmWave including a blockage model between S and D, while [40] considers a multi-hop half duplex over dedicated short range communications (DSRC). In addition, we analyze the outage probability and the throughput, while [40] studies routing strategies for packet forwarding. Finally, the channels are modeled as Nakagami-m fading channels in our analysis. To the best of the authors' knowledge, no previous work has presented a mathematical model for V2V full duplex communications considering the aforementioned scenario. Taking these parameters into consideration, it is clear that the present work differs significantly from previous studies that neither provide analytical outage probability nor throughput expressions. Our main contributions in this work can be summarized as follows:

- Consider the performance analysis of an FDR V2V system over Nakagami$-m$ fading channels.
- Develop a new CDF expression of the ratio of two Gamma distribution random variables (RVs) for the source-relay (S-R) link including self-interference.
- Analyzes and compares two cooperative schemes with full duplex relaying: i) SI vehicle relaying selection and ii) ISI vehicle relaying selection.
- Present the probability of a blockage model between the source and the destination nodes according to independent vehicles Poisson distribution.
- Derive the outage probability with respect to the occurrence of LOS and NLOS probabilistic models, and then obtaining the throughput of the proposed system.

The remainder of this paper is organized as follows: Section II represents the system model. A deep performance analysis of the proposed system is introduced in Section III. Section IV contains numerical and simulation results, and concluding remarks are presented in Section V. Proofs are provided in appendices.

II. V2V FULL DUPLEX COMMUNICATION SYSTEM MODEL

In this paper, we consider a system model composed of one source vehicle S, one destination vehicle D and multiple relay vehicles that are distributed in each lane inside the

[1] In our terminology, we use the term *individual* for the second selection scheme to distinguish between the two proposed selection schemes, as will be mentioned in upcoming sections

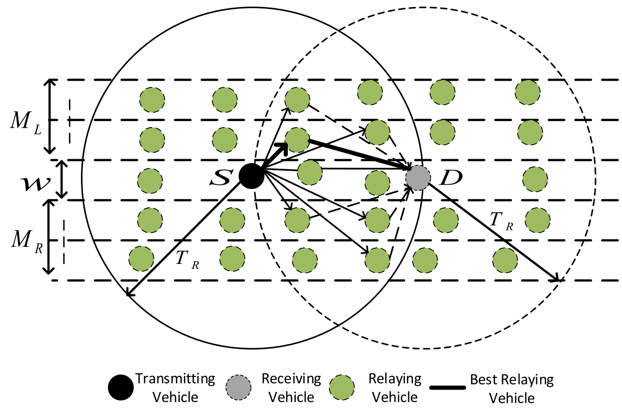

FIGURE 1. **A schematic diagram of the V2V full duplex wireless cooperation multi-lane highway with a transmitter and a receiver located at the central lane, at the existence of left and right lanes.**

transmission range T_R. In our model, all vehicles such as cars, vans, lorries, and buses are located on M parallel traffic lanes with a fixed width of w for each lane. Homogeneous traffic lanes are assumed for simplicity of the analysis, i.e. each traffic lane has an infinite length and an equal number of vehicles. The transmitting vehicle under the analysis has M_L and M_R traffic lanes on its left-hand and right-hand sides respectively, where $M = M_L + M_R + 1$ as shown in Fig. 1. Moreover, the source and the destination are assumed to be placed on the same traffic lane that is called the central lane.[2] Without loss of generality, each vehicle has the same transmitted power P within T_R. The intensity of vehicles in each traffic lane is δ vehicles/lane/unit length and can be represented as $\Psi_\alpha = \{v_{\alpha\beta}; \beta = 0, 1, 2, ...\}$, the lane index $\alpha = 1, 2, ..., M$, and $v_{\alpha\beta}$ denotes the location of the β^{th} vehicle on the α^{th} traffic lane. All the nodes including S, D and the relays are supplied with two antennas, where the transmitter uses only the transmit antenna, the receiver uses only the receive antenna and the vehicle relay nodes use both transmit and receive antennas concurrently to accomplish full duplex relaying.

In the S-D communication link, we consider two cases. The first case assumes the availability of LOS and a direct link is attained. The second case assumes NLOS because the S-D link is obstructed. In our model, it is possible for vehicles to change lane according to independent Poisson distribution. For the cooperation process, a one-way full duplex transmission, taking into account the effect of the residual self-interference at the relay nodes is considered helping S to convey data to D. In addition, we assume that CSIs are also known at the destination node and SC technique is employed to select the best vehicle relay that achieves the highest SNR. Therefore, the best relaying vehicle cooperates only in relaying and one channel is required regardless of the number of vehicle relays.

[2]The central lane means that the transmitting vehicle and the receiving vehicle are located in the same lane to allow direct communication where possible

As mentioned in [46], the SC technique has two important advantages over regular cooperative diversity network i) it reduces the inefficient amount of used channel resources to the best relay node ii) it maintains the full diversity order. Moreover, the SC is implemented in vehicular communication to decrease the number of costly radio frequency (RF) chains at the receiver side, where only a single RF chain needs to be employed at both the transmitter and the receiver nodes [36].

In this vein, we list our system model assumptions

Assumption 1: A dense network in a single direction highway situation at rush hours or in an accident/congestion scenario is considered. Hence, the effect of mobility and the Doppler phenomenon are justifiably ignored. As such, the whole system compromised of the transmitter, the receiver, and the vehicular relays, all move along the same direction on the highway. Any occurrence of a non-zero bias in the Doppler spectrum is compensated by using an automatic frequency control loop at the receiver side [2].

Assumption 2: As shown in Fig. 1, transmitters (source and relays) have a range, T_R, much higher than the highway width, as they should be able to communicate with various infrastructures such as road signs and buildings located across the highway.

Assumption 3: In particular, mmWave is very sensitive to blockage, therefore, LOS is lost if at least one vehicle obstructs the S-D link.

Assumption 4: The Nakagami-m fading channel model is considered as it is widely used to model cooperative vehicular communication and short-range communications [2], [42]. On the other hand, self-interference and its fading model heavily depend on the employed isolation/cancellation techniques. For instance, if the suppression is not sufficiently employed, LOS effects will persist and, hence, Rayleigh-fading will not be a suitable model since it does not count the LOS component. Moreover, the Nakagami$-m$ fading is able to span a wide range of fading distributions that can also capture either scenarios in case of absence/presence of LOS effects. Furthermore, the Nakagami$-m$ distribution is a more general model which can be used to describe many fading distributions such as Rician, Rayleigh or fading environment that is more severe than Rayleigh fading distribution [47].

Furthermore, the average number of relaying vehicles in the highway inside the T_R surrounding the source S can be written as [40]

$$E[|N|] = \delta \left(T_R + \sum_{f=1}^{M_R} \sqrt{T_R^2 - (fw)^2} + \sum_{k=1}^{M_L} \sqrt{T_R^2 - (kw)^2} \right), \tag{1}$$

where $E[\cdot]$ is the expectation operator and $|.|$ represents the set cardinality. In the proposed system model, both R_i, where $i \in \{1, ..., \mathbb{E}[|N|]\}$ and D receive the message transmitted from S, where R_i employs the AF technique and then forwards the message to the destination node. Thus, the received signal at the relay node is composed of the signal emitted by the source plus self-interference. This is expressed as

$$y_{SR_iR_i} = \sqrt{P_S} h_{SR_i} x_S + \sqrt{P_{R_i}} h_{R_iR_i} x_{R_i} + n_{R_i}, \tag{2}$$

where x_S and $x_{R_i} \in \{+1, -1\}$ are the transmitted BPSK symbol signal with unit power, while P_S and P_{R_i} are the transmitted signal power at S and R_i, respectively. The parameters h_{SR_i} and $h_{R_iR_i}$ represent the channel coefficients in the S-R_i link and the self-interference R_i-R_i, respectively. The term n_{R_i} represents white Gaussian noise (AWGN) at R_i with a variance of $\sigma^2_{R_i}$. The channels are modeled as mutually independent Nakagami$-m$ fading channels and are not necessarily identically distributed (i.n.i.d).

Thus, the communication process can be summarized as follows; 1) The transmitted signal reaches the destination D directly and via cooperative relay nodes. This can be modeled as

$$y_{D_{R_i}} = (1-\varepsilon) y_{D_{R_{i_{\text{dir}}}}} + \varepsilon y_{D_{R_{i_{\text{ind}}}}}, \tag{3}$$

with

$$\varepsilon = \begin{cases} 0 & \text{Presence of LOS }, \\ 1 & \text{Absence of LOS}, \end{cases} \tag{4}$$

where the received signal $y_{D_{R_i}}$ is the resultant of the signal arriving directly $y_{D_{R_{i_{\text{dir}}}}}$ on the S-D link plus the relayed signal $y_{D_{R_{i_{\text{ind}}}}}$. In addition, $y_{D_{R_{i_{\text{ind}}}}}$ and $y_{D_{R_{i_{\text{dir}}}}}$ can be individually expressed as

$$y_{D_{R_{i_{\text{ind}}}}} = \sqrt{P_{R_i}} h_{R_iD} \kappa_i y_{SR_iR_i} + n_D, \tag{5}$$

$$y_{D_{R_{i_{\text{dir}}}}} = \sqrt{P_S} h_{SD} x_S + y_{D_{R_{i_{\text{ind}}}}}, \tag{6}$$

where h_{SD}, h_{R_iD} are the channel coefficients in the S-D and R_i-D links respectively, n_D is white Gaussian noise (AWGN) at D with a variance of σ^2_D and $\kappa_i \leq \sqrt{P_{R_i}/(P_S \left|h_{SR_i}\right|^2 + P_{R_i}\left|h_{R_iR_i}\right|^2 + \sigma^2_{R_i})}$ is the amplification factor for AF relaying.

Finally, to capture the impact of path loss on the system performance, the widely normalized distances model is used as in literature e.g. [48]–[50] with $E(|h_{SR}|^2) = (d_{SD}/d_{SR})^\eta$, $E(|h_{RD}|^2) = (d_{SD}/d_{RD})^\eta$, $E(|h_{RR}|^2) = (d_{SD}/d_{RR})^\eta$ and $E(|h_{SD}|^2) = 1$, where η is the path loss exponent and d_{pq} is the distance between vehicle p and q. Due to the high density of vehicles in each lane, the vehicles act as relays and are divided into two groups between source and destination inside the T_R with different source-relay and relay-destination distances.

III. PERFORMANCE ANALYSIS

In this section, we present an analysis on the end-to-end outage performance and the throughput of the proposed system. First, we recall the PDF expression for the S-R_i link including self-interference from [41] to derive the cumulative distribution function (CDF). Once the CDF is obtained, it is used to derive the outage probability expression for our proposed model in two distinct cases, namely the absence or the presence of a direct S-D link.

1) *PDF of the S-R Link Including Self Interference* Here, we derive the PDF expression for the S-R link including self-interference. According to Eq. (2), the received SINR at the relay node is formulated as

$$\gamma_{SR_iR_i} = \frac{P_S \left|h_{SR_i}\right|^2}{P_{R_i}\left|h_{R_iR_i}\right|^2 + N_o} = \frac{\frac{P_S \left|h_{SR_i}\right|^2}{N_o}}{\frac{P_{R_i}\left|h_{R_iR_i}\right|^2}{N_o} + 1} = \frac{\gamma_{SR_i}}{\gamma_{R_iR_i}+1}, \tag{7}$$

where $\gamma_{SR_i} = P_S \left|h_{SR_i}\right|^2/N_o$ and $\gamma_{R_iR_i} = P_{R_i}\left|h_{R_iR_i}\right|^2/N_o$ are the instantaneous SNR of S-R_i and R_i-R_i (loop interference) links respectively. The channel coefficients in the proposed system are modeled as Nakagami$-m$ distribution, therefore, $\left|h_{ij}\right|^2$ follows gamma distribution. Since the channels are independent and not identically distributed (i.n.i.d), the PDF of γ_{SR_i} and $\gamma_{R_iR_i}$ can be respectively written as

$$f_{\gamma_{SR_i}}(x) = \frac{C_{SR_i}^{m_{SR_i}}}{\Gamma(m_{SR_i})} x^{m_{SR_i}-1} \exp(-x C_{SR_i}), \tag{8}$$

$$f_{\gamma_{R_iR_i}}(x) = \frac{C_{R_iR_i}^{m_{R_iR_i}}}{\Gamma(m_{R_iR_i})} x^{m_{R_iR_i}-1} \exp(-x C_{R_iR_i}), \tag{9}$$

where $\Gamma(z)$ denotes the Gamma function and is given by $\Gamma(z) = \int_0^\infty \exp(-t) t^{z-1} dt$ [51, eq. (8.310.1)], $m_i > 0.5$ is the shape parameter, $C_{ij} = \frac{m_{ij}}{\bar{\gamma}_{ij}}$, $\gamma_{ij} = |h_{ij}|^2 P_i/N_o$ is the instantaneous SNR and $\bar{\gamma}_{ij} = E(\left|h_{ij}\right|^2) P_i/N_o$ is the average SNR. The PDF of the total SINR which is stated in Eq. (7) can be written as [41]

$$f_{\gamma_{SR_iR_i}}(x) = \frac{C_{SR_i}^{m_{SR_i}} C_{R_iR_i}^{m_{R_iR_i}} x^{m_{SR_i}-1} \exp(-x C_{SR_i})}{\Gamma(m_{SR_i})\Gamma(m_{R_iR_i})} \times \sum_{j=0}^{m_{SR_i}} \binom{m_{SR_i}}{j} \frac{\Gamma(m_{R_iR_i}+j)}{(x C_{SR_i} + C_{R_iR_i})^{m_{R_iR_i}+j}}, \tag{10}$$

where $\bar{\gamma}_{SR_i}$ and $\bar{\gamma}_{R_iR_i}$ are the average SNR of the S-R_i and R_i-R_i channels, respectively.

2) *CDF of the S-R Link Including Self Interference* We derive the CDF expression for the S-R_i link including self-interference by using Eq. (10).

Theorem 1: The CDF of $\gamma_{SR_iR_i}$ which represents the ratio of two Gamma-distributed RVs can be written as

$$F_{\gamma_{SR_iR_i}}(x) = 1 - \frac{\exp(C_{R_iR_i})}{\Gamma(m_{SR_i})\Gamma(m_{R_iR_i})} \sum_{j=0}^{m_{SR_i}} \binom{m_{SR_i}}{j} \times \Gamma(m_{R_iR_i}+j) \sum_{q=0}^{m_{SR_i}-1} \binom{m_{SR_i}-1}{q} (-1)^{m_{SR_i}-q-1}$$

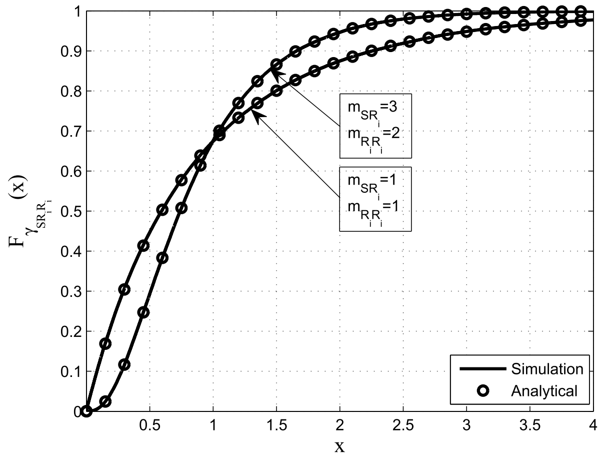

FIGURE 2. Analytical and simulation results for the CDF of SNR of V2V wireless communications in the presence of interference over Nakagami-*m* fading channels for different values of m_{SR_i} and $m_{R_iR_i}$ with $\overline{\gamma}_{SR_i}$ = 2 dB and $\overline{\gamma}_{R_iR_i}$ = 0 dB.

$$\times \left(C_{R_iR_i}\right)^{m_{SR_i}+m_{R_iR_i}-q-1} \times \Gamma\left(q - m_{R_iR_i} - j + 1, \left(C_{SR_i}x + C_{R_iR_i}\right)\right), \quad (11)$$

where $\Gamma(x, y)$ is the upper incomplete Gamma function [51, eq. (8.350.2)]

Proof: See Appendix A

Fig. 2 depicts the CDF results for different values of the fading parameter m_{SR_i} and $m_{R_iR_i}$ at $\overline{\gamma}_{SR_i} = 2$ dB dB and $\overline{\gamma}_{R_iR_i} = 0$ dB, where a perfect match between theoretical expressions and simulation is observed.

3) *Outage Probability*

In this article, we analyze the outage probability of the best vehicular relaying selection of FDR cooperative wireless communications in a dense multi-lane highway situation. We define the outage probability as the probability that the end-to-end SNR between the transmitted signal at the source and the received signal at the destination is smaller than a predefined threshold $\gamma_{th} = 2^{R_T} - 1$, where R_T is the fixed source transmission rate in bits/sec/Hz. The end-to-end outage probabilities are combination of the outage probabilities of the cooperative V2V network in the presence or absence of a direct *S-D* link which are derived in the following subsections A, B, and C.

A. INDIRECT LINK OUTAGE PROBABILITY

In this subsection, a direct link between source and destination nodes is assumed unavailable, a practical situation which arises when at least one vehicle in the central lane blocks a direct *S-D* communication. In addition, a selection combining technique is applied at the destination node to select the best relaying vehicle which offers the highest SNR. Therefore, The instantaneous SNR of the received signal at the destination and using AF relaying technique at the relay node can be written as [52]

$$\gamma_i = \frac{\frac{\frac{P_S|h_{SR_i}|^2}{N_o}}{\frac{P_{R_i}|h_{R_iR_i}|^2}{N_o}+1}\frac{P_{R_i}|h_{R_iD}|^2}{N_o}}{\frac{\frac{P_S|h_{SR_i}|^2}{N_o}}{\frac{P_{R_i}|h_{R_iR_i}|^2}{N_o}+1}+\frac{P_{R_i}|h_{R_iD}|^2}{N_o}+1} = \frac{\gamma_{SR_iR_i}\gamma_{R_iD}}{\gamma_{SR_iR_i}+\gamma_{R_iD}+1} \quad (12)$$

where $\gamma_{R_iD} = P_{R_i}\left|h_{R_iD}\right|^2/N_o$. In addition, a selection combining technique is applied at the destination node to select the best relaying vehicle which offers the highest SINR. Therefore, the total SINR at the destination can be written as [53]

$$\gamma^{sc}_{\text{ind}_{\text{exact}}} = \max_{i\in\{1,\ldots,\mathbb{E}[|N|]\}}(\gamma_i), \quad (13)$$

Since the derivation of the exact outage probability of the two FDR schemes, SI and ISI, is difficult to obtain directly from Eq. (13), then max-min criteria will be used as an alternative to derive the outage probabilities bounds of these latter schemes

1) MAX-MIN CRITERIA OF SI SCHEME (MMSI) WHEN THE S-D LINK IS BLOCKED

The overall SNR in Eq. (13) can be written mathematically as an upper bound expression to calculate the total SNR simply as

$$\gamma^{sc}_{\text{ind}_{\text{MMSI}}} = \max_{i\in\{1,\ldots,\mathbb{E}[|N|]\}}(\min(\gamma_{SR_iR_i}, \gamma_{R_iD})), \quad (14)$$

where $\gamma^{sc}_{\text{ind}_{\text{MMSI}}}$ represents the total SNR at D for indirect links using selection combining technique and $\gamma^{sc}_{\text{ind}_{\text{MMSI}}} \geq \gamma^{sc}_{\text{ind}_{\text{exact}}}$, its accurate to catch the system performance at medium and high SNR. Also, $\gamma_{SR_iR_i}$ represents the SINR at the relay node including the FD loop interference.

Theorem 2: The lower bound of the outage probability for the proposed system including indirect links can be written as

$$P_{\text{ind}_{\text{MMSI}}}(\gamma_{th}) = \sum_{k=0}^{\mathbb{E}[|N|]}\binom{\mathbb{E}[|N|]}{k}(-1)^{\mathbb{E}[|N|]-k}(T_1)^{\mathbb{E}[|N|]-k} \times \left[\exp(-\gamma_{th}C_{R_iD})\sum_{h=0}^{m_{R_iD}-1}\frac{(\gamma_{th}C_{R_iD})^h}{h!}\right]^{\mathbb{E}[|N|]-k}$$

$$T_1 = \frac{\exp(C_{R_iR_i})}{\Gamma(m_{SR_i})\Gamma(m_{R_iR_i})}\sum_{j=0}^{m_{SR_i}}\binom{m_{SR_i}}{j} \times \Gamma(m_{R_iR_i}+j)\sum_{q=0}^{m_{SR_i}-1}\binom{m_{SR_i}-1}{q}(-1)^{m_{SR_i}-q-1}$$

$$\times \left(C_{R_iR_i}\right)^{m_{SR_i}+m_{R_iR_i}-q-1} \times \Gamma\left(q-m_{R_iR_i}-j+1, \left(C_{SR_i}\gamma_{th}+C_{R_iR_i}\right)\right). \quad (15)$$

Note, all the parameters are defined previously.

Proof: See Appendix B

2) MAX-MIN CRITERIA OF ISI SCHEME (MMISI) WHEN THE S-D LINK IS BLOCKED

This technique requires the knowledge of the CSI for the source-relay, relay-relay and relay-destination links separately. The SNR given in Eq. (13) can be further simplified to ease the computation of the PDF of SNR, and can be approximated as

$$\gamma^{sc}_{ind_{MMISI}} = \max_{i\in\{1,\ldots,\mathbb{E}[|N|]\}} (\min(\gamma_{SR_i}, \gamma_{R_iR_i}, \gamma_{R_iD})). \quad (16)$$

The SNR in Eq. (16) represents the lower bound on SNR of MMSI and $\gamma^{sc}_{ind_{MMISI}} \geq \gamma^{sc}_{ind_{MMISI}} \geq \gamma^{sc}_{ind_{exact}}$. As mentioned earlier, the self-interference can not be perfectly eliminated but can be estimated, therefore $\gamma_{R_iR_i}$ represents the residual self-interference (loop interference) after the mitigation process.

Theorem 3: The lower bound of the outage probability for the proposed system including indirect links can be written as

$$P_{ind_{MMISI}}(\gamma_{th}) = \sum_{k=0}^{\mathbb{E}[|N|]} \binom{\mathbb{E}[|N|]}{k} (-1)^{\mathbb{E}[|N|]-k} (T_2)^{\mathbb{E}[|N|]-k}$$

$$T_2 = \frac{\Gamma(m_{SR_i}, \gamma_{th}C_{SR_i})}{\Gamma(m_{SR_i})} \frac{\Gamma(m_{R_iR_i}, \gamma_{th}C_{R_iR_i})}{\Gamma(m_{R_iR_i})} \times \frac{\Gamma(m_{R_iD}, \gamma_{th}C_{R_iD})}{\Gamma(m_{R_iD})}. \quad (17)$$

Following the same steps as in Appendix B, the lower bound on the outage probability of the MMISI when *S-D* is blocked in Eq. (17) can be derived.

B. DIRECT LINK OUTAGE PROBABILITY

In this subsection, a direct *S-D* link is assumed available, a situation that occurs if there is no vehicle in the central lane between the source and destination nodes. In addition, a selection combining technique is applied at the destination node for the two schemes MMSI and MMISI, to choose the best relaying vehicle. Therefore, the total SNR at the destination can be written as

$$\gamma^{sc}_{dir_{exact}} = \max_{i\in\{1,\ldots,\mathbb{E}[|N|]\}} (\gamma_{SD}, \gamma_i). \quad (18)$$

The total outage probability may be derived for two cases as follows

1) MAX-MIN CRITERIA OF SI SCHEME (MMSI) WHEN THE S-D LINK IS AVAILABLE

The overall SNR in Eq. (18) can be expressed as an upper bound to calculate the total SNR as

$$\gamma^{sc}_{dir_{MMSI}} = \max_{i\in\{1,\ldots,\mathbb{E}[|N|]\}} (\gamma_{SD}, \min(\gamma_{SR_iR_i}, \gamma_{R_iD})), \quad (19)$$

where $\gamma^{sc}_{dir_{MMSI}}$ is the total SNR at the destination node for selection combining and $\gamma^{sc}_{dir_{MMSI}} \geq \gamma^{sc}_{dir_{exact}}$. In addition, the SNR in (19) represents an upper bound which is more attractable than the exact SNR in (18).

Theorem 4: The lower bound of the outage probability for the proposed system including direct and indirect links may be written as

$$P_{dir_{MMSI}}(\gamma_{th}) = \left[1-\exp(-\gamma_{th}C_{SD})\sum_{l=0}^{m_{SD}-1}\frac{(\gamma_{th}C_{SD})^l}{l!}\right] \times \sum_{k=0}^{\mathbb{E}[|N|]} \binom{\mathbb{E}[|N|]}{k} (-1)^{\mathbb{E}[|N|]-k} (T_1)^{\mathbb{E}[|N|]-k} \times \left[\exp(-\gamma_{th}C_{R_iD})\sum_{h=0}^{m_{R_iD}-1}\frac{(\gamma_{th}C_{R_iD})^h}{h!}\right]^{\mathbb{E}[|N|]-k} \quad (20)$$

where T_1 is defined previously in Eq. (15)

Proof: See Appendix C

2) MAX-MIN CRITERIA OF ISI SCHEME (MMISI) WHEN THE S-D LINK IS AVAILABLE

This technique requires the knowledge of all CSI pertinent to source-destination, source-relay, relay-relay and relay-destination links separately for estimation process. The SNR in Eq. (18) can be reformulated to simplify the calculation of the PDF of SNR and can be expressed as

$$\gamma^{sc}_{dir_{MMISI}} = \max_{i\in\{1,\ldots,\mathbb{E}[|N|]\}} (\gamma_{SD}, \min(\gamma_{SR_i}, \gamma_{R_iR_i}, \gamma_{R_iD})). \quad (21)$$

The SNR in Eq. (21) represents a lower bound on the SNR of MMSI and $\gamma^{sc}_{dir_{MMSI}} \geq \gamma^{sc}_{dir_{MMSI}} \geq \gamma^{sc}_{dir_{exact}}$

Theorem 5: Following the same steps as in Appendix C, the lower bound on the outage probability of the proposed system including direct *S-D* and indirect links can be written as

$$P_{dir_{MMISI}}(\gamma_{th}) = \left(1-\exp(-\gamma_{th}C_{SD})\sum_{l=0}^{m_{SD}-1}\frac{(\gamma_{th}C_{SD})^l}{l!}\right) \times \sum_{k=0}^{\mathbb{E}[|N|]} \binom{\mathbb{E}[|N|]}{k} (-1)^{\mathbb{E}[|N|]-k} (T_2)^{\mathbb{E}[|N|]-k}, \quad (22)$$

where T_2 is defined previously in Eq. (17).

C. END-TO-END OUTAGE PROBABILITY

Theorem 6: The end-to-end outage probability of MMIS or MMISI systems ($P_{\text{e2e}_{\text{MMSI/MMISI}}}(\gamma_{th})$) can be found using the combination of direct and indirect links including the probability of blockage P_c as follows

$$P_{\text{e2e}_{\text{MMSI/MMISI}}}(\gamma_{th}) = P_c P_{\text{ind}_{\text{MMSI/MMISI}}}(\gamma_{th}) + (1-P_c) P_{\text{dir}_{\text{MMSI/MMISI}}}(\gamma_{th}), \tag{23}$$

where $P_{\text{ind}_{\text{MMSI}}}(\gamma_{th})$, $P_{\text{dir}_{\text{MMSI}}}(\gamma_{th})$, $P_{\text{ind}_{\text{MMISI}}}(\gamma_{th})$, and $P_{\text{dir}_{\text{MMISI}}}(\gamma_{th})$ are defined in Eq. (15), Eq. (20), Eq. (17) and Eq. (22) respectively and P_c represents the probability that there exists a vehicle inside the central lane (probability of blockage) that can be calculated as follows

$$\begin{aligned} P_c &= P[\text{At least one vehicle in the central lane}] \\ &= 1 - P[\text{No vehicle in the central lane}] \\ &= 1 - \exp(-\delta T_R). \end{aligned} \tag{24}$$

Substituting Eq. (15), Eq. (20) and Eq. (24) into Eq. (23), $P_{\text{e2e}_{\text{MMSI}}}(\gamma_{th})$ can be written as in Eq. (25), shown at the bottom of the next page.

Theorem 7: In order to find the end-to-end outage probability of MMISI system, Eq. (17), Eq. (22) and Eq. (24) are simply plugged into Eq. (23) to yield $P_{\text{e2e}_{\text{MMISI}}}(\gamma_{th})$ as in Eq. (26), shown at the bottom of the next page.

4) *Throughput*

In this subsection, we present the throughput performance of FD V2V wireless cooperative AF relaying. The throughput of the MMIS and MMISI systems are defined as the total number of packÉTS that are successfully delivered to the receiver with no error for a given period of time in bits/sec/Hz and can be written as [54]

$$G = R_T(1 - P_{\text{e2e}_{\text{MMSI/MMISI}}}(\gamma_{th})), \tag{27}$$

where R_T is the fixed rate of the transmitter in bits/sec/Hz.

IV. SIMULATION RESULTS

Analytical and simulation results for the outage probability and throughput of the proposed system are delivered in this section.

The system simulation setup includes the transmission of 10^6 bits, a lane width of $w = 0.04$, $M = 5$ traffic lanes with $M_R = M_L = 2$, a transmission range of $T_R = 1$, and a path loss exponent of $\eta = 3.18$. Moreover, the vehicles in each lane are distributed with the intensity of $\delta = 2$ vehicles/lane/unit length. Hence, vehicles acting as relays inside the transmission range are assumed to be present in symmetrical locations around the central lane. As mentioned earlier, relaying vehicles are divided into two groups between S and D within the range T_R with different distances. The distances of the first group are $d_{SR_i} = 0.4$ and $d_{R_iD} = 0.6$, respectively, and that of the second group are $d_{SR_i} = 0.7$ and $d_{R_iD} = 0.3$, respectively, with $d_{SD} = 1$ and $d_{R_iR_i} = 0.01$. Therefore, we have $d_{SR_i} + d_{R_iD} = 1$. For simplicity, the transmission power is set to $P_S = P_R = P$. All the exact simulation results are compared to MMSI and MMISI schemes in Eq. (25) and Eq. (26) respectively in the case of outage probability and also compared to the throughput in Eq. (27). Furthermore, some corresponding case-specific system parameters are included in the caption of each figure, where applicable.

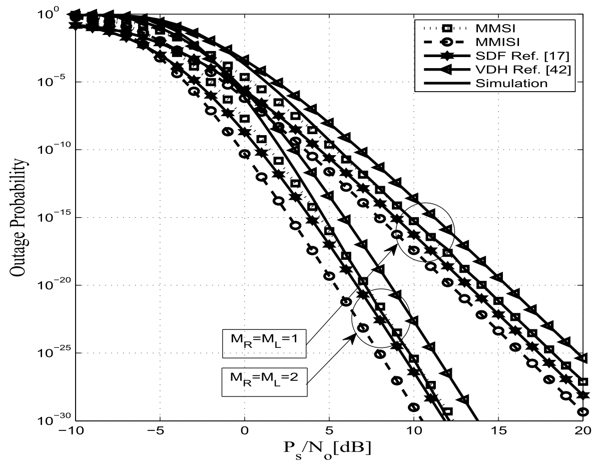

FIGURE 3. Analytical and simulation results for the outage probability vs. P_S/N_o of V2V wireless communications in the presence of interference over Nakagami−m fading channels for different values of M_R and M_L, $m_{ij} = 2$, where $i, j \in \{S, R, D\}$, $\delta = 2$ vehicles/lane/unit length, $w = 0.04$, $T_R = d_{SD} = 1$, $d_{SR_i} = 0.4$ and 0.7, $d_{R_iD} = 0.6$ and 0.3, respectively, $d_{R_iR_i} = 0.01$, $\overline{\gamma}_{R_iR_i} = 0$ dB, $R_T = 1$ bit/sec/Hz and $\eta = 3.18$.

Fig. 3 depicts the evaluation of the outage probability for the best vehicle relaying selection as a function of P_S/N_o with a different number of highway lanes. As can be seen, the performance improvement is proportional to the number of highway lanes. For instance, an outage probability of 10^{-10} appears at $\approx$ 0 dB when the total number of lanes $M = 5$, while it occurs at $\approx$ 3.5 dB for $M = 3$ lanes in the MMISI scheme. For the MMSI structure, however, an outage probability of 10^{-10} appears at $\approx$ 1.5 dB for $M = 5$ lanes, while it occurs at $\approx$ 5.2 dB for $M = 3$. For exact simulation, the outage probability of 10^{-10} occurs at $\approx$ 2.3 dB for $M = 5$ and at $\approx$ 5.3 dB for $M = 3$ lanes. This behavior is mathematically described in Eq. (1) in the paper, where expanding the highway to contain more lanes increases the average number of vehicular relays inside the transmission range and improves performance.

Furthermore, our results Fig. 3 are compared to vehicular full duplex dual hop scheme (VDH) which represented in [42]. It is clear that the outage probability derived in this paper is better than that proposed in [42] with $\approx$ 1 dB diversity gain at medium and high P_S/N_o in both cases of $M = 5$ and $M = 3$ lanes for MMSI and simulation results. The degradation of VDH scheme due to the self-interference at the relay node and also because the direct link is seen as interference at the destination node. For example, an outage probability of 10^{-15} occurs at $\approx$ 4.5 dB and at $\approx$ 10 dB for $M = 5$ and for $M = 3$ lanes respectively, while it occurs at

$\approx$ 5.6 dB and at $\approx$ 11 dB for the same number of lanes in VDH scheme [42].

Moreover, our results are also compared to selective DF (SDF) full duplex relaying [17] which is also known as vehicular full duplex joint decoding (VJD) [41]. As observed, SDF has a better outage probability performance compared to the MMSI scheme. This degradation in MMSI scheme is due to the effect of blockage probability on the system performance as shown in Eq. (25).

As for the outage probability, Fig. 4 shows the outage probability of the best relaying vehicle as a function of the P_S/N_o. The obtained results are compared to exact simulation under different fading values m_{ij} in full duplex mode including self-interference, over i.n.i.d Nakagami$-m$ fading channels. It is clear that as m_{ij}, where $i, j \in \{S, R, D\}$ values increase, the outage probability decreases significantly and the performance improves. On the other hand, higher m_{SD} values do not enhance the system performance due to the high density of vehicles in the central lane that also causes a high blockage probability of the direct link. More, it can be observed that the derived lower bound on MMSI is close enough to the exact simulation result, especially at medium and high P_S/N_o values, and is valid for different values of m_{ij}. For example, the outage probability for the exact simulation for $m_{ij} = 2$ at $P_S/N_o = 8$ dB is equal to 4.2×10^{-22} while the outage probability for the MMSI is equal to 2.6×10^{-22} and for MMISI 7.9×10^{-26}. At the same time the outage probability at $m_{ij} = 3$ for exact simulation equals to 6.1×10^{-31}, for MMSI is equal to 1.5×10^{-31} and for MMISI is 1.3×10^{-36}. On the other hand, a gap of approximated 2 dB is observed at high SNR between the simulation results and the MMISI scheme. This gap is because the MMISI takes into account the effect of the self-interference individually and does not mingle it into the relay input as represented in Eq. (16) and Eq. (21).

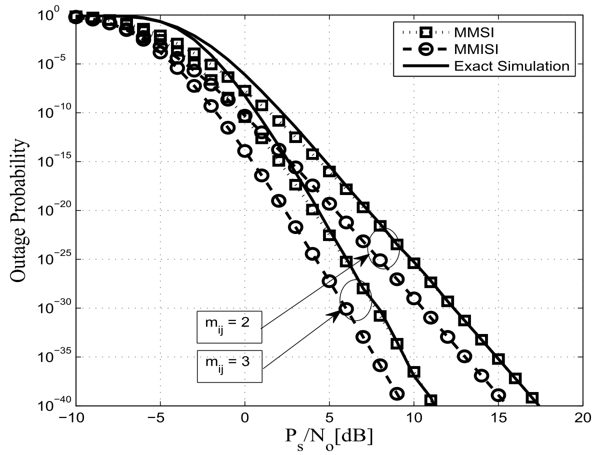

FIGURE 4. Analytical and simulation results for the outage probability vs. P_S/N_o of V2V wireless communications in the presence of interference over Nakagami$-m$ fading channels for different values of m_{ij}, where $i, j \in \{S, R, D\}$, $R_T = 1$ bit/sec/Hz, $\delta = 2$ vehicles/lane/unit length, $w = 0.04$, $M_R = M_L = 2$, $T_R = d_{SD} = 1$, $d_{SR_i} = 0.4$ and 0.7, $d_{R_iD} = 0.6$ and 0.3, respectively, $d_{R_iR_i} = 0.01$, $\overline{\gamma}_{R_iR_i} = 0$ dB and $\eta = 3.18$.

Fig. 5 plots the outage probability in Eq. (25) and Eq. (26) as a function of P_S/N_o for different source transmission rates R_T. Also, the results of the lower bounds are verified by the exact simulation for the parameters indicated in the caption. While this figure clearly exhibits the closeness of our analytical expressions and simulation results for medium

$$P_{e2e_{MMSI}}(\gamma_{th}) = \sum_{k=0}^{\mathbb{E}[|N|]} \binom{\mathbb{E}[|N|]}{k} (-1)^{\mathbb{E}[|N|]-k} \left[\frac{\exp(C_{R_iR_i})}{\Gamma(m_{SR_i})\Gamma(m_{R_iR_i})}\right]^{\mathbb{E}[|N|]-k} \left[\sum_{j=0}^{m_{SR_i}} \binom{m_{SR_i}}{j} \Gamma(m_{R_iR_i}+j)\right]^{\mathbb{E}[|N|]-k}$$
$$\times \left[\sum_{q=0}^{m_{SR_i}-1} \binom{m_{SR_i}-1}{q} (-1)^{m_{SR_i}-q-1} \left(C_{R_iR_i}\right)^{m_{SR_i}+m_{R_iR_i}-q-1} \Gamma\left(q - m_{R_iR_i} - j + 1, \left(C_{SR_i}\gamma_{th} + C_{R_iR_i}\right)\right)\right]^{\mathbb{E}[|N|]-k}$$
$$\times \left[\exp(-\gamma_{th}C_{R_iD}) \sum_{h=0}^{m_{R_iD}-1} \frac{(\gamma_{th}C_{R_iD})^h}{h!}\right]^{\mathbb{E}[|N|]-k}$$
$$\times \left[(1-\exp(-\delta T_R)) + \exp(-\delta T_R)\left(1 - \exp(-\gamma_{th}C_{SD}) \sum_{l=0}^{m_{SD}-1} \frac{(\gamma_{th}C_{SD})^l}{l!}\right)\right] \quad (25)$$

$$P_{e2e_{MMISI}}(\gamma_{th}) = \sum_{k=0}^{\mathbb{E}[|N|]} \binom{\mathbb{E}[|N|]}{k} (-1)^{\mathbb{E}[|N|]-k} \left(\frac{\Gamma(m_{SR_i}, \gamma_{th}C_{SR_i})}{\Gamma(m_{SR_i})} \frac{\Gamma(m_{R_iR_i}, \gamma_{th}C_{R_iR_i})}{\Gamma(m_{R_iR_i})} \frac{\Gamma(m_{R_iD}, \gamma_{th}C_{R_iD})}{\Gamma(m_{R_iD})}\right)^{\mathbb{E}[|N|]-k}$$
$$\times \left[(1-\exp(-\delta T_R)) + \exp(-\delta T_R)\left(1 - \exp(-\gamma_{th}C_{SD}) \sum_{l=0}^{m_{SD}-1} \frac{(\gamma_{th}C_{SD})^l}{l!}\right)\right] \quad (26)$$

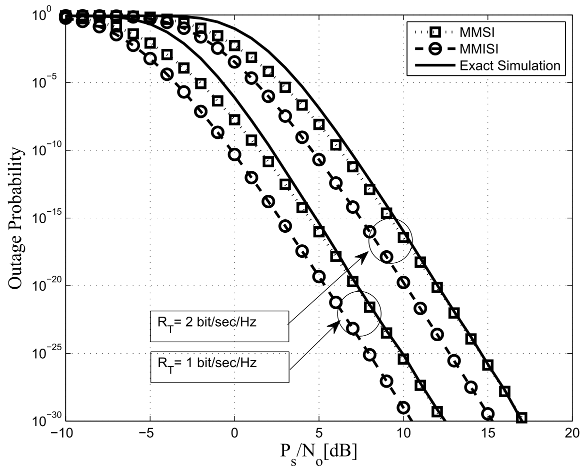

FIGURE 5. Analytical and simulation results for the outage probability vs. P_S/N_o of V2V wireless communications in the presence of interference over Nakagami−m fading channels for different values of R_T, $m_{ij} = 2$, where $i, j \in \{S, R, D\}$, $\delta = 2$ vehicles/lane/unit length, $w = 0.04$, $M_R = M_L = 2$, $T_R = d_{SD} = 1$, $d_{SR_i} = 0.4$ and 0.7, $d_{R_iD} = 0.6$ and 0.3, respectively, $d_{R_iR_i} = 0.01$, $\overline{\gamma}_{R_iR_i} = 0$ dB and $\eta = 3.18$.

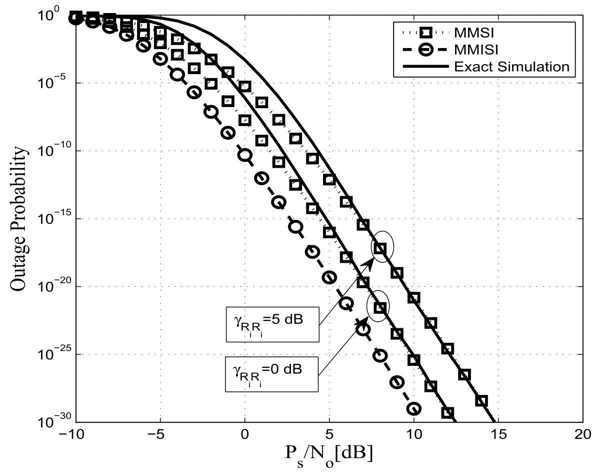

FIGURE 6. Analytical and simulation results for the outage probability vs. P_S/N_o of V2V wireless communications in the presence of interference over Nakagami−m fading channels for different values of $\overline{\gamma}_{R_iR_i}$, $m_{ij} = 2$, where $i, j \in \{S, R, D\}$, $\delta = 2$ vehicles/lane/unit length, $w = 0.04$, $M_R = M_L = 2$, $T_R = d_{SD} = 1$, $d_{SR_i} = 0.4$ and 0.7, $d_{R_iD} = 0.6$ and 0.3, respectively, $d_{R_iR_i} = 0.01$, $d_{R_iR_i} = 0.01$, $R_T = 1$ bit/sec/Hz and $\eta = 3.18$.

and high P_S/N_o values, an important point we could deduce from it is that the performance improves with less R_T as expected. As an example, the outage probability of 10^{-10} occurs at $\approx$ 1.5 dB in the case of $R_T = 1$ bit/sec/Hz, while it occurs at $\approx$ 6.3 dB in the case of $R_T = 2$ bit/sec/Hz for the MMSI scheme. However, the outage probability of 10^{-10} occurs at $\approx$ 0 dB in the case of $R_T = 1$ bit/sec/Hz, while it occurs at $\approx$ 4.5 dB in the case of $R_T = 2$ bit/sec/Hz for the MMISI scheme. For the exact simulation result, the outage probability of 10^{-10} occurs at $\approx$ 2.3 dB and $\approx$ 6.8 dB in the case of $R_T = 1$ and $R_T = 2$ bit/sec/Hz respectively. This behavior can be explained as follows: Decreasing the source transmission rate R_T cuts back the threshold value, which allows more relays to participate in forwarding the information to the destination node and improve the performance by reducing the outage probability. In addition, it can be seen in Fig. 4 and Fig. 5 that the lower bound on MMSI and the exact simulation approach are close enough to each other as P_S/N_o increases while the two curves dissociate at low P_S/N_o values. In consequence, the total SNR expressions provided in Eq. (14) and Eq. (19) have a higher accuracy for larger P_S/N_o values.

Fig. 6 shows the performance of the best vehicle relaying scheme under several values of the average self-interference at relay nodes. We observe a deterioration of the system performance, i.e. an augmentation of the outage probability while the average self-interferences at the relays increase. This result validates our theoretical analysis as narrated by Eq. (7), where the destructive influence of the self-interference on the outage probability as an important measure of the system performance is clearly indicated. the capacity of the proposed system is controlled by the ratio $(\gamma_{SR_i}/\gamma_{R_iR_i}+1)$ at high SNR regime and thus the lower bound agrees with the exact simulation for high P_S/N_o values. Based on the aforementioned reason, using an interference

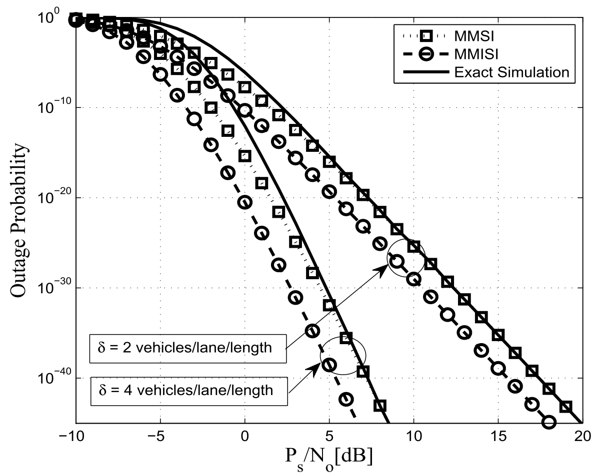

FIGURE 7. Analytical and simulation results for the outage probability vs. P_S/N_o of V2V wireless communications in the presence of interference over Nakagami−m fading channels for different values of δ, $M_R = M_L = 2$, $m_{ij} = 2$, where $i, j \in \{S, R, D\}$, $w = 0.04$, $T_R = d_{SD} = 1$, $d_{SR_i} = 0.4$ and 0.7, $d_{R_iD} = 0.6$ and 0.3, respectively, $d_{R_iR_i} = 0.01$, $\overline{\gamma}_{R_iR_i} = 0$ dB, $R_T = 1$ bit/sec/Hz and $\eta = 3.18$.

cancellation scheme at relaying nodes in the full duplex mode reduces interference and enhances system performance. In this figure, the diversity gain between MMISI and MMSI is $\approx$ 2 dB and $\approx$ 4 dB for $\overline{\gamma}_{R_iR_i} = 0$ dB and 5 dB respectively. Moreover, the MMISI performance shows no change with respect to self-interference because the latter is treated separately.

Fig. 7 depicts a comparison of the outage probabilities for the approximated theoretical expressions versus simulation results under the different intensity of vehicles in each traffic lane. As the situation intensifies from *dense* to *ultra dense*, i.e. as the number of vehicles δ increase from 2 to 4 vehicles/lane/unit length, the performance of the proposed

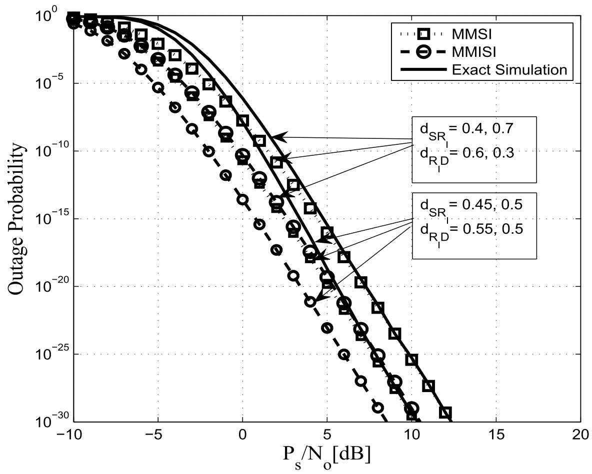

FIGURE 8. Analytical and simulation results for the outage probability vs. P_S/N_O of V2V wireless communications in the presence of interference over Nakagami−m fading channels for different distances between $S - R_i$ and $R_i - D$ links, $M_R = M_L = 2$, $m_{ij} = 2$, where $i, j \in \{S, R, D\}$, $\delta = 2$ vehicles/lane/unit length, $w = 0.04$, $T_R = d_{SD} = 1$, $d_{SR_i} = 0.4$ and 0.7, $d_{R_iD} = 0.6$ and 0.3, respectively, $d_{R_iR_i} = 0.01$, $\bar{\gamma}_{R_iR_i} = 0$ dB, $R_T = 1$ bit/sec/Hz and $\eta = 3.18$.

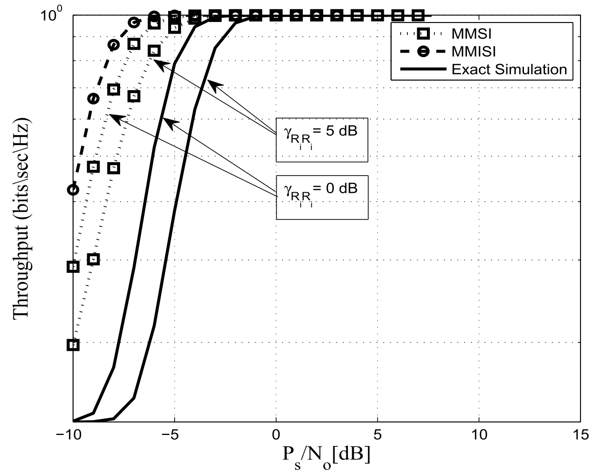

FIGURE 9. Throughput of V2V wireless communications in the presence of interference over Nakagami−m fading channels for different values of $\bar{\gamma}_{R_iR_i}$, $m_{ij} = 2$, where $i, j \in \{S, R, D\}$, $R_T = 1$ bit/sec/Hz, $\delta = 2$ vehicles/lane/unit length, $w = 0.04$, $M_R = M_L = 2$, $T_R = d_{SD} = 1$, $d_{SR_i} = 0.4$ and 0.7, $d_{R_iD} = 0.6$ and 0.3, respectively, $d_{R_iR_i} = 0.01$ and $\eta = 3.18$.

TABLE 1. Blockage Probability.

	$T_R = 1$	$T_R = 0.5$
$\delta = 2$ vehicles/lane/unit length	$P_c = 0.8647$	$P_c = 0.6321$
$\delta = 4$ vehicles/lane/unit length	$P_c = 0.9817$	$P_c = 0.8647$

system improves. Note that the impact of δ and T_R on the blockage probability is significant. This can be explained as follows, increasing the intensity of vehicles per lane including the central lane from $\delta = 2$ to 4 augments the blockage probability as shown in Table 1 and further obstructs the LOS. However, more selections of the *best relaying vehicle* become available within T_R to process relaying. In addition, we observe that the blockage probability does not swiftly change over the time. This is because it depends on δ, which changes very slowly in dense environments. Fig. 8 exhibits the performance of the proposed system in terms of the outage probability with different distances between $S-R_i$ and R_i-D links. It is clear from the figure that relaying vehicles enhance the system performance more effectively if located in the middle zone between the source and the destination, as this situation indicates a balanced average channel gain between $S - R_i$ and $R_i - D$ links. As we can see, if the relaying vehicles are placed in the middle zone between source and destination such that they observe balanced distances such as $d_{SR_i} = 0.45, 0.5$ and $d_{R_iD} = 0.55$ and 0.45, the system performance slightly improves and the outage probability decreases compared to cases where $d_{SR_i} = 0.4, 0.7$ and $d_{R_iD} = 0.6$ and 0.3.

Figs. 9-10 illustrate the throughput for V2V AF dual-hop wireless cooperative communications for the best vehicular relay selection versus P_S/N_o. Fig. 9 exhibits the destructive influence of self-interference at vehicular relays on the throughput. As seen, the throughput of the proposed system is higher for less self-interference. Fig. 10 shows the improvement of the throughput when the number of lanes around the central lane is increased. This is because more adjacent lanes provide potentially more vehicular relays inside the transmission range, which enhances throughput. For example, when the number of lanes $M_R = M_L = 2$, the system accomplishes a high throughput at ≈ -5 dB while reducing the number of lanes to $M_R = M_L = 1$, then ≈ -4 dB is required to achieve the same throughput in the MMISI scheme. In the MMIS scheme, however, the throughput reaches its peak at ≈ -4 dB for $M_R = M_L = 2$ and at ≈ -3 dB for $M_R = M_L = 1$ lanes. As wider highways with more lanes around the central lane provide space for more potential vehicular relays, the overall system throughput is expected to grow on such infrastructure.

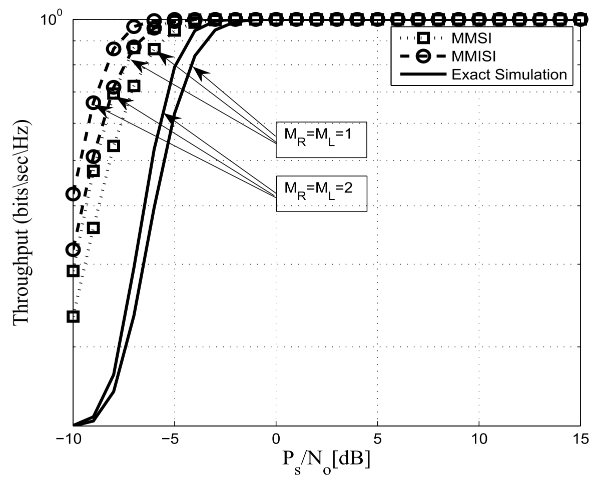

FIGURE 10. Throughput of V2V wireless communications in the presence of interference over Nakagami−m fading channels for different values of M_R and M_L, $m_{ij} = 2$, where $i, j \in \{S, R, D\}$, $R_T = 1$ bit/sec/Hz, $\delta = 2$ vehicles/lane/unit length, $w = 0.04$, $T_R = d_{SD} = 1$, $d_{SR_i} = 0.4$ and 0.7, $d_{R_iD} = 0.6$ and 0.3, respectively, $d_{R_iR_i} = 0.01$, $\bar{\gamma}_{R_iR_i} = 0$ dB and $\eta = 3.18$.

V. CONCLUSIONS

A V2V full duplex AF cooperative wireless network model was presented. Two dissimilar vehicular relay selection schemes in a dense multi-lane highway over Nakagami$-m$ fading channels were proposed in the absence/presence of LOS. In addition, vehicle displacement from one lane to an adjacent lane has taken place according to independent Poisson distribution. One of the selection schemes introduced in this work took into account the source-relay and the relay-relay links by one CSI coefficient, while the other one considered the effect of the self-interference individually and did not mingle it into the relay input. The vehicular relay selection schemes were evaluated in terms of the outage probability and the throughput. Our results indicate that, the MMSI provides a lower bound that is very close to the exact simulation results, especially at medium and high SNR, and the MMISI is simple to derive mathematically. Our analytical derivations revealed the trade-off between these two selection schemes based on the purpose of the application. We derived closed-form expressions for the CDF of the SINR and used it to develop the end-to-end outage probability. The end-to-end outage probability was derived based on the blockage probability in the central lane. The system performance was analyzed and studied in various scenarios from several aspects, including fading severity, threshold, self-interference, number of lanes, the intensity of vehicles in each traffic lane, and inter-vehicle spacing. Indeed, this paper provided a comprehensive benchmark for measuring the performance of evolving V2V full duplex relaying in cooperative wireless networks.

APPENDIX A

The CDF of $\gamma_{SR_iR_i}$ can be attained as

$$F_{\gamma_{SR_iR_i}}(\gamma_{th}) = \int_0^{\gamma_{th}} f_{\gamma_{SR_iR_i}}(x)dx = 1 - \int_{\gamma_{th}}^{\infty} f_{\gamma_{SR_iR_i}}(x)dx. \quad (28)$$

Substituting Eq. (10) into Eq. (28), we get

$$F_{\gamma_{SR_iR_i}}(x) = 1 - \frac{C_{SR_i}^{m_{SR_i}} C_{R_iR_i}^{m_{R_iR_i}}}{\Gamma(m_{SR_i})\Gamma(m_{R_iR_i})} \times \sum_{j=0}^{m_{SR_i}} \binom{m_{SR_i}}{j} \frac{\Gamma(m_{R_iR_i}+j)}{(C_{SR_i})^{m_{R_iR_i}+j}} \times \underbrace{\int_{\gamma_{th}}^{\infty} \frac{x^{m_{SR_i}-1}\exp(-xC_{SR_i})}{(x+\frac{C_{R_iR_i}}{C_{SR_i}})^{m_{R_iR_i}+j}} dx}_{I_1}. \quad (29)$$

Solving the integral (I_1) to obtain the CDF by letting $g = x+z$ and $z = \frac{C_{R_iR_i}}{C_{SR_i}}$

$$\int_{\gamma_{th}+z}^{\infty} \frac{(g-z)^{m_{SR_i}-1}\exp(-(g-z)C_{SR_i})}{g^{m_{R_iR_i}+j}} dg. \quad (30)$$

Adopting the binomial theorem, expands $(g-z)^{m_{SR_i}-1}$ as

$$(g-z)^{m_{SR_i}-1} = \sum_{q=0}^{m_{SR_i}-1} \binom{m_{SR_i}-1}{q} (-1)^{m_{SR_i}-1-q} \times z^{m_{SR_i}-1-q} g^q. \quad (31)$$

Substituting Eq. (31) into Eq. (30) results in

$$I_1 = \exp(C_{R_iR_i}) \sum_{q=0}^{m_{SR_i}-1} \binom{m_{SR_i}-1}{q} (-1)^{m_{SR_i}-1-q} \times z^{m_{SR_i}-1-q} \underbrace{\int_{\gamma_{th}+z}^{\infty} g^{q-m_{R_iR_i}-j-1} \exp(-C_{SR_i} g) dg}_{I_2}. \quad (32)$$

Using [51, eq. (3.381.3)] produces

$$I_2 = C_{SR_i}^{-q+m_{R_iR_i}+j-1} \times \Gamma\left(q - m_{R_iR_i} - j + 1, \left(C_{SR_i}x + C_{R_iR_i}\right)\right). \quad (33)$$

Finally, making $z = \frac{C_{R_iR_i}}{C_{SR_i}}$, $x = \gamma_{th}$, substituting Eq. (33) into Eq. (32), and then in Eq. (29) will complete the proof of Eq. (11)

APPENDIX B

The outage probability of the proposed system including indirect S-D links can be written as

$$P_{\text{ind}_{\text{MMSI}}}(\gamma_{th}) = P(\gamma_{\text{ind}_{\text{total}}}^{\text{sc}} \le \gamma_{th}). \quad (34)$$

Substituting Eq. (14) into Eq. (34)

$$P_{\text{ind}_{\text{MMSI}}}(\gamma_{th}) = P[\max_{i\in\{1,\ldots,\mathbb{E}[|N|]\}} [\min(\gamma_{SR_iR_i}, \gamma_{R_iD})]]. \quad (35)$$

In addition, $P_{\gamma_{SR_iR_iD}}(\gamma_{th})$ can be expressed as

$$P_{\gamma_{SR_iR_iD}}(\gamma_{th}) = P_{\min(\gamma_{SR_iR_i},\gamma_{R_iD})}(\gamma_{th}) = 1 - [1 - P_{\gamma_{SR_iR_i}}(\gamma_{th})][1 - P_{\gamma_{R_iD}}(\gamma_{th})] \quad (36)$$

where $P_{\gamma_{SR_iR_i}}(\gamma_{th})$ is defined in Eq. (11) and

$$P_{\gamma_{R_iD}}(\gamma_{th}) = \frac{\gamma(m_{R_iD}, \gamma_{th}C_{R_iD})}{\Gamma(m_{R_iD})}. \quad (37)$$

Substituting Eq. (11) and Eq. (37) into Eq. (36) results in Eq. (38) that represents the outage probability of one S-R_i-R_i-D link including self-interference at the relay node.

$$P_{\gamma_{SR_iR_iD}}(\gamma_{th}) = 1 - \left[T_1 \frac{\Gamma(m_{R_iD}, \gamma_{th}C_{R_iD})}{\Gamma(m_{R_iD})}\right], \quad (38)$$

where T_1 is defined in Eq. (15)

To generalize the analytical expression obtained in Eq. (38), multi-vehicular relays are included. Doing so yields

$$P_{\text{ind}_{\text{MMSI}}}(\gamma_{th}) = \prod_{i=1}^{\mathbb{E}[|N|]} P_{\gamma_{SR_iR_iD}}(\gamma_{th}). \quad (39)$$

Substituting Eq. (38) into Eq. (39) yields the outage probability for the proposed system with indirect S-D as

$$P_{\text{ind}_{\text{MMSI}}}(\gamma_{th}) = \prod_{i=1}^{\mathbb{E}[|N|]} 1 - \left[T_1 \frac{\Gamma(m_{R_iD}, \gamma_{th} C_{R_iD})}{\Gamma(m_{R_iD})} \right]. \quad (40)$$

It is then possible to derive the outage probability for the proposed system with indirect links as follows:

From [51, eqs. (8.352.4) and (8.339.1)], we have

$$\frac{\Gamma(m_{R_iD}, \gamma_{th} C_{R_iD})}{\Gamma(m_{R_iD})} = \exp(-\gamma_{th} C_{R_iD}) \sum_{h=0}^{m_{R_iD}-1} \frac{(\gamma_{th} C_{R_iD})^h}{h!}. \quad (41)$$

Utilizing [51, Eq. (1.111)] and substituting Eq. (41) into Eq. (40), reduces to Eq. (15), that concludes the proof.

APPENDIX C

The outage probability in this case is derived using $\max(\gamma_{SD}, \gamma_{SR_iR_iD})$ and is expressed as

$$P_{\text{dir}_{\text{MMSI}}}(\gamma_{th}) = P[\max_{i \in \{1,\ldots,\mathbb{E}[|N|]\}} (\gamma_{SD}, \gamma_{SR_iR_iD}) \leq \gamma_{th}]. \quad (42)$$

which can rewritten as

$$P_{\text{dir}_{\text{MMSI}}}(\gamma_{th}) = P_{\gamma_{SD}}(\gamma_{th}) \times P_{\text{ind}_{\text{MMSI}}}(\gamma_{th}), \quad (43)$$

where $P_{\text{ind}_{\text{MMSI}}}(\gamma_{th})$ is obtained previously in Eq. (15), and

$$P_{SD}(\gamma_{th}) = \frac{\gamma(m_{SD}, \gamma_{th} C_{SD})}{\Gamma(m_{SD})}. \quad (44)$$

with $\gamma(x, y) = \int_0^y t^{x-1} e^{-t} dt$ being the lower incomplete Gamma function [51, eq. (8.350.1)]. From [51, eq. (8.352.6)], we have

$$\frac{\gamma(m_{SD}, \gamma_{th} C_{SD})}{\Gamma(m_{SD})} = \left[1 - \exp(-\gamma_{th} C_{SD}) \sum_{l=0}^{m_{SD}-1} \frac{(\gamma_{th} C_{SD})^l}{l!} \right]. \quad (45)$$

Eq. (20) is obtained by substituting Eq. (15) and Eq. (45) into Eq. (43).

REFERENCES

[1] X. Yang, L. Liu, N. H. Vaidya, and F. Zhao, "A vehicle-to-vehicle communication protocol for cooperative collision warning," in *Proc. MobiQuitous*, 2004, pp. 114–123.
[2] A. Tassi, M. Egan, R. J. Piechocki, and A. Nix, "Modeling and design of millimeter-wave networks for highway vehicular communication," *IEEE Trans. Veh. Technol.*, vol. 66, no. 12, pp. 10676–10691, Dec. 2017.
[3] A. Ghosh *et al.*, "Millimeter-wave enhanced local area systems: A high-data-rate approach for future wireless networks," *IEEE J. Sel. Areas Commun.*, vol. 32, no. 6, pp. 1152–1163, Jun. 2014.
[4] K. N. Qureshi and A. H. Abdullah, "A survey on intelligent transportation systems," *Middle-East J. Sci. Res.*, vol. 15, no. 5, pp. 629–642, 2013.
[5] C. Campolo, A. Molinaro, A. O. Berthet, and A. Vinel, "Full-duplex radios for vehicular communications," *IEEE Commun. Mag.*, vol. 55, no. 6, pp. 182–189, Jun. 2017.
[6] C. M. Silva, B. M. Masini, G. Ferrari, and I. Thibault, "A survey on infrastructure-based vehicular networks," *Mobile Inf. Syst.*, vol. 2017, Aug. 2017, Art. no. 6123868.
[7] D. Kim, H. Lee, and D. Hong, "A survey of in-band full-duplex transmission: From the perspective of PHY and MAC layers," *IEEE Commun. Surveys Tuts.*, vol. 17, no. 4, pp. 2017–2046, 4th Quart., 2015.
[8] M. Duarte and A. Sabharwal, "Full-duplex wireless communications using off-the-shelf radios: Feasibility and first results," in *Proc. Conf. Rec. 40th Asilomar Conf. Signals Syst. Comput. (ASILOMAR)*, Nov. 2010, pp. 1558–1562.
[9] M. Jain *et al.*, "Practical, real-time, full duplex wireless," in *Proc. Int. Conf. Mobile Comput. Netw.*, 2011, pp. 301–312.
[10] D. Qin, Y. Wang, and T. Zhou, "Average SEP of AF relaying in Nakagami-fading environments," *Wireless Commun, Mobile Comput.*, vol. 2018, 2018, Art. no. 6581827.
[11] M. K. Shukla, S. Yadav, and N. Purohit, "Performance evaluation and optimization of traffic-aware cellular multiuser two-way relay networks over Nakagami-*m* fading," *IEEE Syst. J.*, vol. 12, no. 2, pp. 1933–1944, Jun. 2018.
[12] N. Kumar, P. K. Singya, and V. Bhatia, "Performance analysis of orthogonal frequency division multiplexing-based cooperative amplify-and-forward networks with non-linear power amplifier over independently but not necessarily identically distributed Nakagami-*m* fading channels," *IET Commun.*, vol. 11, no. 7, pp. 1008–1020, 2017.
[13] S. Qian, X. Zhou, X. He, J. He, M. Juntti, and T. Matsumoto, "Performance analysis for lossy-forward relaying over Nakagami-*m* fading channels," *IEEE Trans. Veh. Technol.*, vol. 66, no. 11, pp. 10035–10043, Nov. 2017.
[14] H. Alves, G. Fraidenraich, R. D. Souza, M. Bennis, and M. Latva-Aho, "Performance analysis of full duplex and selective and incremental half duplex relaying schemes," in *Proc. IEEE Wireless Commun. Netw. Conf.*, Apr. 2012, pp. 771–775.
[15] T. Kwon, S. Lim, S. Choi, and D. Hong, "Optimal duplex mode for DF relay in terms of the outage probability," *IEEE Trans. Veh. Technol.*, vol. 59, no. 7, pp. 3628–3634, Sep. 2010.
[16] H. Alves, D. B. da Costa, R. D. Souza, and M. Latva-Aho, "Performance of block-Markov full duplex relaying with self interference in Nakagami-*m* fading," *IEEE Wireless Commun. Lett.*, vol. 2, no. 3, pp. 311–314, Jun. 2013.
[17] M. G. Khafagy, A. Ismail, M.-S. Alouini, and S. Aíssa, "Efficient cooperative protocols for full-duplex relaying over Nakagami-*m* fading channels," *IEEE Trans. Wireless Commun.*, vol. 14, no. 6, pp. 3456–3470, Jun. 2015.
[18] P. K. Sharma and P. Garg, "Outage analysis of full duplex decode and forward relaying over Nakagami-*m* channels," in *Proc. NCC*, New Delhi, India, Feb. 2013, pp. 1–5.
[19] A. Almradi and K. A. Hamdi, "On the outage probability of MIMO full-duplex relaying: Impact of antenna correlation and imperfect CSI," *IEEE Trans. Veh. Technol.*, vol. 66, no. 5, pp. 3957–3965, May 2017.
[20] S. Li *et al.*, "Full-duplex amplify-and-forward relaying: Power and location optimization," *IEEE Trans. Veh. Technol.*, vol. 66, no. 9, pp. 8458–8468, Sep. 2017.
[21] I. Krikidis, H. A. Suraweera, P. J. Smith, and C. Yuen, "Full-duplex relay selection for amplify-and-forward cooperative networks," *IEEE Trans. Wireless Commun.*, vol. 11, no. 12, pp. 4381–4393, Dec. 2012.
[22] N. Kothapalli, P. Sharma, and V. Kumar, "Performance of a bi-directional relaying system with one full duplex relay," *AEU-Int. J. Electron. Commun.*, vol. 70, no. 10, pp. 1426–1432, 2016.
[23] H. Cui, M. Ma, L. Song, and B. Jiao, "Relay selection for two-way full duplex relay networks with amplify-and-forward protocol," *IEEE Trans. Wireless Commun.*, vol. 13, no. 7, pp. 3768–3777, Jul. 2014.
[24] Y. Wang, Y. Xu, N. Li, W. Xie, K. Xu, and X. Xia, "Relay selection of full-duplex decode-and-forward relaying over Nakagami-*m* fading channels," *IET Commun.*, vol. 10, no. 2, pp. 170–179, Feb. 2016.
[25] M. Gaafar, M. G. Khafagy, O. Amin, R. F. Schaefer, and M.-S. Alouini, "Full-duplex relaying with improper Gaussian signaling over Nakagami-*m* fading channels," *IEEE Trans. Commun.*, vol. 66, no. 1, pp. 64–78, Jan. 2018.
[26] Y. Ai and M. Cheffena, "Performance analysis of hybrid-ARQ over full-duplex relaying network subject to loop interference under Nakagami-*m* fading channels," in *Proc. IEEE Veh. Technol. Conf. (VTC Spring)*, Jun. 2017, pp. 1–5.
[27] H. Fu, S. Roy, and J. Cheng, "Applying Hankel's expansion for performance analysis in double-Nakagami (generalized-k) fading channels," *IEEE Trans. Commun.*, vol. 66, no. 10, pp. 4893–4906, Oct. 2018.
[28] H. Ilhan, I. Altunbas, and M. Uysal, "Cooperative diversity for relay-assisted inter-vehicular communication," in *Proc. IEEE VTC Spring*, May s2008, pp. 605–609.

[29] Z. Li, Y. Zhao, H. Chen, and H. Hu, ''Outage probability bound analysis in vehicle-assisted inter-vehicular communications,'' in *Proc. IEEE 14th Int. Conf. Comput. Supported Cooperat. Work Design (CSCWD)*, Apr. 2010, pp. 783–787.

[30] A. I. Akin, H. Ilhan, and Ö. Özdemir, ''Relay selection for DF-based cooperative vehicular systems,'' *EURASIP J. Wireless Commun. Netw.*, vol. 2015, no. 1, pp. 1–9, 2015.

[31] H. Ilhan, M. Uysal, and I. Altunbas, ''Cooperative diversity for intervehicular communication: Performance analysis and optimization,'' *IEEE Trans. Veh. Technol.*, vol. 58, no. 7, pp. 3301–3310, Sep. 2009.

[32] S. Q. Nguyen and H. Y. Kong, ''Outage probability analysis in dual-hop vehicular networks with the assistance of multiple access points and vehicle nodes,'' *Wireless Pers. Commun.*, vol. 87, no. 4, pp. 1175–1190, 2016.

[33] P. S. Bithas, G. P. Efthymoglou, and A. G. Kanatas, ''Intervehicular communication systems under co-channel interference and outdated channel estimates,'' in *Proc. IEEE Int. Conf. Commun. (ICC)*, Kuala Lumpur, Malaysia, May 2016, pp. 1–6.

[34] H. Ilhan, ''Performance analysis of cooperative vehicular systems with co-channel interference over cascaded Nakagami-*m* fading channels,'' *Wireless Pers. Commun.*, vol. 83, no. 1, pp. 203–214, 2015.

[35] Y. Alghorani, G. Kaddoum, S. Muhaidat, S. Pierre, and N. Al-Dhahir, ''On the performance of multihop-intervehicular communications systems over *n** Rayleigh fading channels,'' *IEEE Wireless Commun. Lett.*, vol. 5, no. 2, pp. 116–119, Apr. 2016.

[36] Y. Alghorani and M. Seyfi, ''On the performance of reduced-complexity transmit/receive-diversity systems over MIMO-V2V channel model,'' *IEEE Wireless Commun. Lett.*, vol. 6, no. 2, pp. 214–217, Apr. 2017.

[37] R. Shakeri, H. Khakzad, A. Taherpour, and S. Gazor, ''Performance of two-way multi-relay inter-vehicular cooperative networks,'' in *Proc. IEEE Wireless Commun. Netw. Conf. (WCNC)*, Apr. 2014, pp. 520–525.

[38] Y. Hu, H. Li, C. Zhang, and J. Li, ''Partial relay selection for a roadside-based two-way amplify-and-forward relaying system in mixed Nakagami-*m* and double Nakagami-*m* fading,'' *IET Commun.*, vol. 8, no. 5, pp. 571–577, 2014.

[39] G. T. Pitsiladis, D. Papanikolaou, A. D. Panagopoulos, and C. Antoniou, ''Vehicle-to-vehicle communication: End-to-end performance evaluation in dense propagation environments,'' in *Proc. IEEE 9th Eur. Antennas Propag. Conf.*, May 2015, pp. 1–5.

[40] M. J. Farooq, H. ElSawy, and M.-S. Alouini, ''A stochastic geometry model for multi-hop highway vehicular communication,'' *IEEE Trans. Wireless Commun.*, vol. 15, no. 3, pp. 2276–2291, Mar. 2016.

[41] K. Eshteiwi, K. Ben Fredj, G. Kaddoum, and F. Gagnon, ''Performance analysis of peer-to-peer V2V wireless communications in the presence of interference,'' in *Proc. IEEE 26th Annu. Int. Symp. Pers., Indoor, Mobile Radio Commun. (PIMRC)*, Sep. 2017, pp. 1–6.

[42] S. B. Mafra, E. M. Fernandez, and R. D. Souza, ''Performance analysis of full-duplex cooperative communication in vehicular ad-hoc networks,'' *IFAC-Papers OnLine*, vol. 49, no. 30, pp. 227–232, 2016.

[43] M. Khafagy, A. Ismail, M.-S. Alouini, and S. Aissa, ''On the outage performance of full-duplex selective decode-and-forward relaying,'' *IEEE Commun. Lett.*, vol. 17, no. 6, pp. 1180–1183, Jun. 2013.

[44] A. Bazzi, A. Zanella, and B. M. Masini, ''Performance analysis of V2V beaconing using LTE in direct mode with full duplex radios,'' *IEEE Wireless Commun. Lett.*, vol. 4, no. 6, pp. 685–688, Dec. 2015.

[45] T. Yang, R. Zhang, X. Cheng, and L. Yang, ''A graph coloring resource sharing scheme for full-duplex cellular-VANET heterogeneous networks,'' in *Proc. IEEE Int. Conf. Comput. Netw. Commun. (ICNC)*, Feb. 2016, pp. 1–5.

[46] S. S. Ikki and M. H. Ahmed, ''Performance of multiple-relay cooperative diversity systems with best relay selection over Rayleigh fading channels,'' *EURASIP J. Adv. Signal Process.*, vol. 2008, no. 1, 2008, Art. no. 580368.

[47] L. Cheng, B. E. Henty, D. D. Stancil, F. Bai, and P. Mudalige, ''Mobile vehicle-to-vehicle narrow-band channel measurement and characterization of the 5.9 GHz dedicated short range communication (DSRC) frequency band,'' *IEEE J. Sel. Areas Commun.*, vol. 25, no. 8, pp. 1501–1516, Oct. 2007.

[48] J. N. Laneman, D. N. C. Tse, and G. W. Wornell, ''Cooperative diversity in wireless networks: Efficient protocols and outage behavior,'' *IEEE Trans. Inf. Theory*, vol. 50, no. 12, pp. 3062–3080, Dec. 2004.

[49] S. S. Ikki and M. H. Ahmed, ''Performance analysis of decode-and-forward incremental relaying cooperative-diversity networks over Rayleigh fading channels,'' in *Proc. IEEE 26th Annu. Int. Symp. Pers., Indoor, Mobile Radio Commun. (PIMRC)*, Apr. 2009, pp. 1–6.

[50] H. Lateef, D. C. McLernon, and M. Ghogho, ''Performance analysis of cooperative communications with opportunistic relaying,'' in *Proc. IEEE Int. Workshop Signal Process. Adv. Wireless Commun. (SPAWC)*, Jun. 2010, pp. 1–5.

[51] A. Jeffrey and D. Zwillinger, *Table of Integrals, Series, and Products*. New York, NY, USA: Academic, 2007.

[52] M. O. Hasna and M. S. Alouini, ''Outage probability of multihop transmission over Nakagami fading channels,'' *IEEE Commun. Lett.*, vol. 7, no. 5, pp. 216–218, May 2003.

[53] S. S. Soliman and N. C. Beaulieu, ''Exact analysis of dual-hop AF maximum end-to-end SNR relay selection,'' *IEEE Trans. Commun.*, vol. 60, no. 8, pp. 2135–2145, Aug. 2012.

[54] M. G. Khafagyx, M. S. Alouini, and S. Aïssa, ''On the performance of future full-duplex relay selection networks,'' in *Proc. IEEE CAMAD*, Sep. 2015, pp. 11–16.

KHALED ESHTEIWI received the B.Sc. degree in electrical engineering (communications) from the Higher Institute for Electronics, Bani Walid, Libya, in 2002, the master's degree in communications engineering from the Academy of Postgraduate Studies, Tripoli, Libya, in 2006, and the M.Sc. degree from Concordia University, Montreal, QC, Canada, in 2014. He has been doing his Ph.D. research studies at the Electrical Engineering Department, École de Technologie Supérieure, University of Quebec, Canada. His current research interests include wireless communications, telecommunications, cooperative wireless communications, and relaying networks.

GEORGES KADDOUM (M'11) received the bachelor's degree in electrical engineering from the École Nationale Supérieure de Techniques Avancées, Brest, France, the M.S. degree in telecommunications and signal processing from the Université de Bretagne Occidentale and Telecom Bretagne (ENSTB), Brest, in 2005, and the Ph.D. degree (Hons.) in signal processing and telecommunications from the National Institute of Applied Sciences, Université de Toulouse, Toulouse, France, in 2009. He is currently an Associate Professor and the Research Chair of electrical engineering with the École de Technologie Supérieure (ÉTS), University of Quebec, Montreal, QC, Canada. Since 2010, he has been a Scientific Consultant in the field of space and wireless telecommunications for several U.S. and Canadian companies. In 2014, he was awarded the ÉTS Research Chair in physical-layer security for wireless networks. He has published over 150 journal and conference papers and has two pending patents. His recent research interests include mobile communication systems, modulations, security, and space communications and navigation. He received the Best Papers Awards from the 2014 IEEE International Conference on Wireless and Mobile Computing, Networking and Communications, with three coauthors, and the 2017 IEEE International Symposium on Personal Indoor and Mobile Radio Communications, with four coauthors. He received the 2015 and 2017 IEEE Transactions on Communications Exemplary Reviewer Award, the Research Excellence Award from the Université du Québec, in 2018, and the Research Excellence Award from the ÉTS, in 2019. He serves as an Associate Editor for the IEEE Transactions on Information Forensics and Security and the IEEE Communications Letters.

KAIS BEN FREDJ (S'08–M'12) was born in Tunis, Tunisia. He received the Diplome National d'Ingenieur (B.Sc.) degree from the Higher School of Communications, in 2006, and the M.Sc. and Ph.D. degrees in telecommunications from INRS, Université du Québec, in 2009 and 2014, respectively. His research interests include resource allocation, OFDMA, cognitive radio, spectrum sharing, performance analysis in fading, shadowing, and composite channels, and physical network coding. He has received an Excellency Grant from the Ministry of Communications, during his B.Sc and Ph.D. studies in Canada. He was a recipient of the Tunisian Government Excellency Scholarship, from 2007 to 2012.

EBRAHIM SOUJERI (M'03–SM'11) received the B.Sc., M.Sc., and Ph.D. degrees in electrical and electronics engineering from Eastern Mediterranean University (EMU), Famagusta, Northern Cyprus, in 1995, 1997, and 2003, respectively, and the Ph.D. degree from the École de Technologie Supérieure, Montreal, QC, Canada, in 2018. He was with the Department of Electrical and Electronics Engineering, EMU, from 1996 to 2002, as a Research Assistant. In 2002, he taught at the Department of Computer Engineering, Cyprus International University. In 2003, he joined the Faculty of Engineering, European University of Lefke, Northern Cyprus. In 2007, he was a Visiting Assistant Professor with Sultan Qaboos University, Muscat, Oman. He has also taught at the Department of Computer Science and Software Engineering, Concordia University, Montreal, Canada, on a part-time basis, from 2012 to 2014. He is currently an Independent Researcher. His research interests include wireless communication systems, spread spectrum, and index modulation techniques. He is a Reviewer of various IEEE journals and conferences.

FRANÇOIS GAGNON (S'87–M'87–SM'99) received the B. Eng. and Ph.D. degrees in electrical engineering from the École Polytechnique de Montréal, Montreal, QC, Canada. He has been a Professor with the Department of Electrical Engineering, École de technologie supérieure (ÉTS), Montreal, since 1991. He was the Director of the Department of Electrical Engineering, from 1999 to 2001. Since 2001, he has been an Industrial Research Chair. In addition to holding the Richard J. Marceau Industrial Research Chair for Wireless Internet in developing countries, he also holds the NSERC-Ultra Electronics Chair in Wireless Emergency and Tactical Communication, the most prestigious industrial chair program in Canada. He also founded the Communications and Microelectronic Integration Laboratory and was its first Director. He has been very actively involved in the creation of the new generation of high-capacity line-of-sight military radios offered by the Canadian Marconi Corporation, which is now Ultra Electronics Tactical Communication Systems. Ultra Electronics TCS and ÉTS have obtained the NSERC Synergy prize for this collaboration. He serves on the boards of funding agencies and companies. He specializes in wireless communications, modulation, coding, microelectronics, signal processing, equalization, software-defined radio, mobile communication, and fading channels. He is actively involved in the SmartLand Project of UTPL, Ecuador, and the STARACOM str.